

AEROSOL MONITORING FROM SPACE USING MODIS AOD MEASUREMENTS
OVER THE JING-JIN-JI REGION OF CHINA DURING 2000-2017

by

Xiqi Fei
A Thesis
Submitted to the
Graduate Faculty
of
George Mason University
in Partial Fulfillment of
The Requirements for the Degree
of
Master of Science
Earth Systems Science

Committee:

_____	Dr. John J. Qu, Thesis Director
_____	Dr. Donglian Sun, Committee Member
_____	Dr. Paul Dirmeyer, Committee Member
_____	Dr. Anthony Stefanidis, Department Chairperson
_____	Dr. Donna M. Fox, Associate Dean, Office of Student Affairs & Special Programs, College of Science
_____	Dr. Peggy Agouris, Dean, College of Science
Date: _____	Summer Semester 2017 George Mason University Fairfax, VA

Aerosol Monitoring from Space Using MODIS AOD Measurements over the Jing-Jin-Ji
Region of China During 2000-2017

A Thesis submitted in partial fulfillment of the requirements for the degree of Master of
Science at George Mason University

by

Xiqi Fei
Bachelor of Engineering
China University of Geosciences, 2015

Director: John J. Qu, Professor
Department of Geography and GeoInformation Science

Spring Semester 2017
George Mason University
Fairfax, VA

Copyright 2017 Xiqi Fei
All Rights Reserved

DEDICATION

This is dedicated to my loving parents and friends.

ACKNOWLEDGEMENTS

First and foremost, I would like to thank my thesis advisor, Dr. John J. Qu, for all his guidance, encouragement and support. I would like to thank my committee members Dr. Donglian Sun and Dr. Paul Dirmeyer for their valuable insight, guidance, and feedback. My sincere thanks to Dr. Xiaojun Hao for his technical guidance.

I would like to thank my parents who have always loved me unconditionally and encouraged me to work hard for the dreams that I aspire to fulfill.

Finally, thanks to my friends for their support throughout the whole process, especially Sindhukumar Sundaram, Jiao Ma, Fang Yi, Ibifubara Iganibo, and David Benson. All you have done are appreciated.

TABLE OF CONTENTS

	Page
List of Tables	vi
List of Figures	vii
List of Equations	viii
List of Abbreviations	ix
Abstract	x
Chapter 1 Introduction	1
Chapter 2 Literature Review	4
Chapter 3 Methodology	7
Section 3.1 Study Area.....	7
Section 3.2 Datasets & Quality assurance.....	9
Section 3.3 Time Series Analysis.....	10
Section 3.4 Spatial Distribution Analysis	12
Section 3.5 Smog Event Detection.....	12
Chapter 4 Data Analysis and Findings.....	14
Section 4.1 Trend and Seasonal Cycle	14
Section 4.2 Spatial Distribution	20
Section 4.3 Air Quality & MODIS 8-Day AOD Product	23
Chapter 5 Conclusions and Discussion.....	28
References	29

LIST OF TABLES

Table	Page
Table 1 The Division of Four Seasons and the Corresponding 8-Day Dataset	11
Table 2 Major cities in the Jing-Jin-Ji region	12
Table 3 Smog events and the duration	13
Table 4 Major cities' AOD mean.....	22
Table 5 The smog event duration, AQI and AOD data time range	23

LIST OF FIGURES

Figure	Page
Figure 1 Location of the Jing-Jin-Ji region in China	7
Figure 2 A natural-color image captured by MODIS on the Aqua satellite(NASA Earth Observatory images by Joshua Stevens).....	8
Figure 3 Grids counted as the Jing-Jin-Ji region	9
Figure 4 Time series of 8-Day MODIS AOD over the Jing-Jin-Ji region.....	14
Figure 5 The mean seasonal cycle of 8-Day MODIS AOD over the Jing-Jin-Ji region. .	15
Figure 6 The STL decomposition of an 8-day AOD time series	16
Figure 7 Comparison between STL Seasonal Component and the Mean Seasonal Cycle	17
Figure 8 The AOD trends of four seasons	18
Figure 9 Boxplot of AOD	19
Figure 10 Grids counted as the Jing-Jin-Ji region	20
Figure 11 Grids selected for specific cities/areas	21
Figure 12 The yearly AOD of four seasons	22
Figure 13 AOD products involved when smog events happened	24
Figure 14 Normalized AQI and AOD.....	26

LIST OF EQUATIONS

Equation	Page
Equation 1 Additive and multiplicative structures for decomposition models	11

LIST OF ABBREVIATIONS

Aerosol Optical Depth	AOD
AErosol RObotic NETwork	AERONET
Air Quality Index	AQI
Earth Observation System.....	EOS
Light Detection and Ranging	LIDAR
Ministry of Environmental Protection of the People's Republic of China	MEP
MODerate Resolution Imaging Spectroradiometer	MODIS
National Aeronautics and Space Administration.....	NASA
Particulate Matter.....	PM
Quality Assurance.....	QA
Seasonal and Trend decomposition using Loess	STL

ABSTRACT

AEROSOL MONITORING FROM SPACE USING MODIS AOD MEASUREMENTS OVER THE JING-JIN-JI REGION OF CHINA DURING 2000-2017

Xiqi Fei, M.S.

George Mason University, 2017

Thesis Director: Dr. John J. Qu

With more severe smog events reported in China, increasing attention has been attached to air quality in China. Aerosols, the minute solid or liquid particles suspended in the atmosphere, have an immense effect on air quality. Satellites Aerosol Optical Depth (AOD) monitoring has the advantage of routinely providing spatial and temporal measurements of aerosol loading in the atmosphere. Using China's Jing-Jin-Ji region as a study area, this thesis seeks to determine whether severe smog events could be detected by the MODIS (MODerate Resolution Imaging Spectroradiometer) 8-day AOD product; and, if there is an increasing tendency of AOD during 2000-2017 in the Jing-Jin-Ji region. Also, the AOD values of major Jing-Jin-Ji cities are compared to get the geographical distribution characteristics of the AOD. The results from this thesis aim to provide a better understanding of AOD characteristics in China's Jing-Jin-Ji region.

CHAPTER 1 INTRODUCTION

With the rapid urbanization and industrialization, China's economy has enjoyed 30 years of high-speed growth. However, the country's relaxed oversight for environment safety during the development process has brought various environmental issues, such as air pollution, water pollution, and soil degradation. Air pollution is one of the major environmental issues (Hao & Wang, 2005), which happens when the air contains gasses, dust, and smoke in harmful amounts. Jing-Jin-Ji ("Jing" for Beijing, "Jin" for Tianjin and "Ji" for the traditional name of Hebei Province), the national capital region located in the center of the economic area of Northern China, is one of the most important regions in the country's economic development plan over the next century (Johnson, 2015). However, air pollution is a big problem there. Compared with most other cities in China, Jing-Jin-Ji has been facing the most severe air pollution situation. According to the report from China's Ministry of Environmental Protection (MEP), only 56.8% of days in the Jing-Jin-Ji region were clear in 2016, and 9.2% of the days were "heavily polluted," much higher than the national average of 2.6% (Zhao, 2017).

With an increasing number of severe air pollution events like smog reported by the social media, there is a lot of public concern about air pollution controls. In response to public pressure and increased pollution, the Chinese government has initiated and implemented a number of national policies to curb air pollution and to improve the

environmental situation across cities and provinces in China (Zhang, He, & Huo, 2012) such as the 12th Five Year Plan, the Air Pollution Prevention and Control (2012) and the 13th Five Year Plan.

Recent reports from government and international organizations show that air quality in China is improving (Fu, Wan, Zhang, & Cheng, 2016; Xie et al., 2015). However, smog events were still frequently happening in the winter of 2016 (November 2016 – January 2017), which seems to disagree with the air quality reports showing improvement. The National Meteorological Center (NMC) of China even issued its first ever red national alert for fog (the highest of four levels) in a number of northern and eastern regions along with renewing an earlier released orange alert (the second-highest level) for haze at the beginning of 2017. According to the China Meteorological Administration official website, the Jing-Jin-Ji region experienced seven moderate or intense smog events from November to December in 2016, having two more smog events compared with the same period in 2016.

All the recent air pollution events and relative reports raise a question as to whether China's air quality is improving. Satellite monitoring data provide information about air quality in terms of Aerosol Optical Depth (AOD). As a function of wavelength λ , AOD describes aerosol's attenuation of light and refers to the integral of aerosol extinction coefficient in the atmospheric vertical path (Kaufman & Fraser, 1983). Therefore, it is a vertically-integrated measure that does not distinguish between lower troposphere, upper troposphere or stratosphere aerosols. The load, shape, and size of aerosols could affect AOD. AOD produced by MODIS (Moderate Resolution Imaging

Spectroradiometer) is able to discern air quality categories (Chu et al., 2003; Wang & Christopher, 2003).

By using the MODIS AOD product, this thesis uses the Jing-Jin-Ji region as a study area to discuss the following questions:

1. How is the air quality issue reflected through satellite monitoring data products?
2. What are the trends and seasonal characteristics of AOD in the Jing-Jin-Ji region during 2000-2017?
3. How was the air pollution distributed in the Jing-Jin-Ji region?

CHAPTER 2 LITERATURE REVIEW

Aerosols are a mixture of solid and liquid particles suspended in the atmosphere. The aerosol produced from the land surface or sea surface through natural processes (such as dust and ocean waves foam) determines most of the aerosols. In the meanwhile, particulate matter and precursor gasses emitted as a result of human activities also have a huge impact on the total amount of aerosols (Andreae & Rosenfeld, 2008).

Aerosols affect climate through direct and indirect effects of radiation. The total direct effect of aerosols is cooling of the atmosphere, but also they could indirectly change microphysical properties of cloud, thus affecting the radiation properties of clouds (Forster et al., 2007). Referred to as Particulate Matter (PM), aerosols also have a significant impact on air quality and human health. In the densely-populated regions, high concentrations of these fine PM have a strong relationship with the early death and shortened life expectancy (Pope, Ezzati, & Dockery, 2009).

Aerosol remote sensing refers to a set of theories and methods used to study aerosol characteristics through satellite or ground-based remote sensing data, which can continuously derive aerosol characteristics. Although ground-based remote sensing by sun photometer can get more accurate observations of aerosol information, this method is limited by its fixed monitoring site, losing the distribution of information. Aerosol monitoring using satellite remote sensing in the global scale could enhance understanding

of aerosol properties of spatial and temporal variations (Lee, Li, Kim, & Kokhanovsky, 2009). Satellite observation has the following four advantages in aerosol monitoring:

1. It can provide large spatial coverage for aerosol measurements.
2. It can continuously observe aerosol information for the long term. Sun-synchronous satellites visit the same location on Earth two times per day, while geostationary satellites continuously observe the same region.
3. It has fewer limitations than the ground measurements. For example, it can easily observe rural areas and over the ocean.
4. It could gain various aerosol information by multi-channel, multi-angle and polarization observations.

In addition, many algorithms and techniques for satellite retrievals of aerosol properties have been developed (King, Kaufman, Tanré, & Nakajima, 1999).

Since AOD products have the highest observation accuracy and are most utilized in observations, it is the most important optical property of aerosols (King, Byrne, Herman, & Reagan, 1978). It is an important factor in the assessment of air quality.

Flying on the Earth Observation System's (EOS) Terra and Aqua satellites, MODIS sensors have been observing the Earth since 2000 and 2002 respectively (Lorraine A. Remer et al., 2008). The MODIS aerosol product monitors the ambient aerosol optical depth globally. During the processing of aerosol products, seven MODIS channels are used for aerosol retrieval (L. A. Remer et al., 2005), and several other wavelengths are used for cloud masking (Ackerman et al., 1998). MODIS Level-2 (L2) aerosol products are produced at the spatial resolution 10×10 km, and the Level-3 (L3)

MODIS daily aerosol products, which contain $1^{\circ} \times 1^{\circ}$ grid values of atmospheric parameters related to aerosol particle properties, are the aggregation result from the L2 product (Platnick, 2015). MODIS L3 8-day and the monthly products are computed from the consecutive L3 daily product files (Hubanks, Platnick, King, & Ridgway, 2016). It is convenient to use MODIS L3 daily, 8-day, or monthly products to conduct an analysis of long-term trends. The previous assessment shows the MODIS AOD L3 is considered valuable (Dudhia, Ruiz-Arias, Gueymard, & Pozo-Vazquez, 2013).

Many previous studies have been done with MODIS AOD products. MODIS L2 daily products have been widely used to assess the relationship with PM_{2.5} air quality (Engel-Cox, Holloman, Coutant, & Hoff, 2004; Wang & Christopher, 2003). MODIS L3 Monthly products were used in studies to investigate AOD at large spatial and temporal scales, like in the study of the AOD trend over the Middle East (Klingmüller, Pozzer, Metzger, Stenchikov, & Lelieveld, 2016) and AOD variability over the Indian Subcontinent (Prasad, Singh, & Singh, 2004).

CHAPTER 3 METHODOLOGY

Section 3.1 Study Area

In this research, the Jing-Jin-Ji region is used as a case study for exploring the long-term trend of AOD and spatial characteristics of AOD distribution in this region.

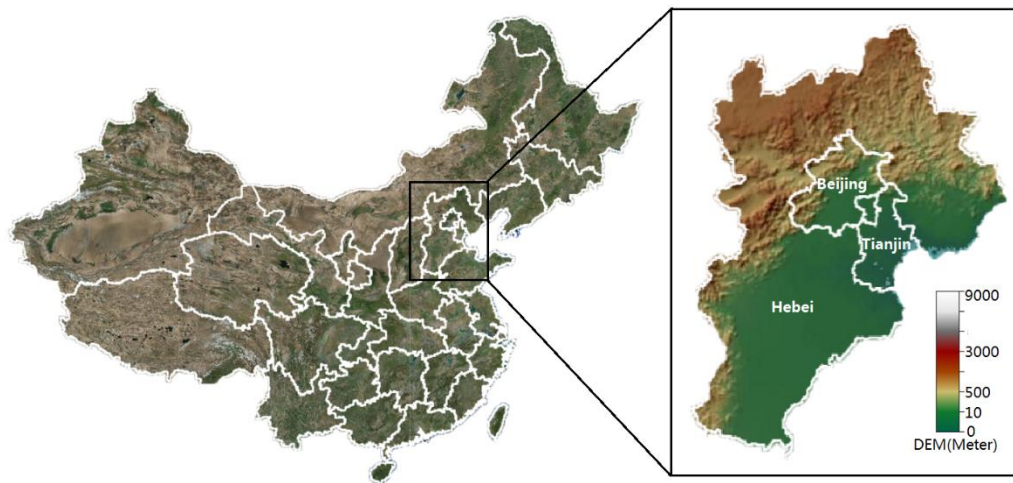


Figure 1 Location of the Jing-Jin-Ji region in China

Located in Northern China, the Jing-Jin-Ji region borders the Bohai Bay on the east. The northern and western sides of the Jing-Jin-Ji region are semi-enclosed by the Taihang Mountains on the west and Yanshan Mountain on the north, while the southern part of the region lies on the North China Plain with elevations less than 50 meters above

sea level. Figure 1 shows a China map along with boundaries of the provinces and a map of the Jing-Jin-Ji region with a Digital Elevation Model (DEM) mosaic as the background. This region has a continental monsoon climate, which is humid and hot in summer and dry cold in winter (Wikipedia). The large-scale smog pollution which is characterized by particulate matter pollutant has frequently accumulated in this region with high concentrations (Ji et al., 2012), especially during the winter dry season (W. Li et al., 2011).

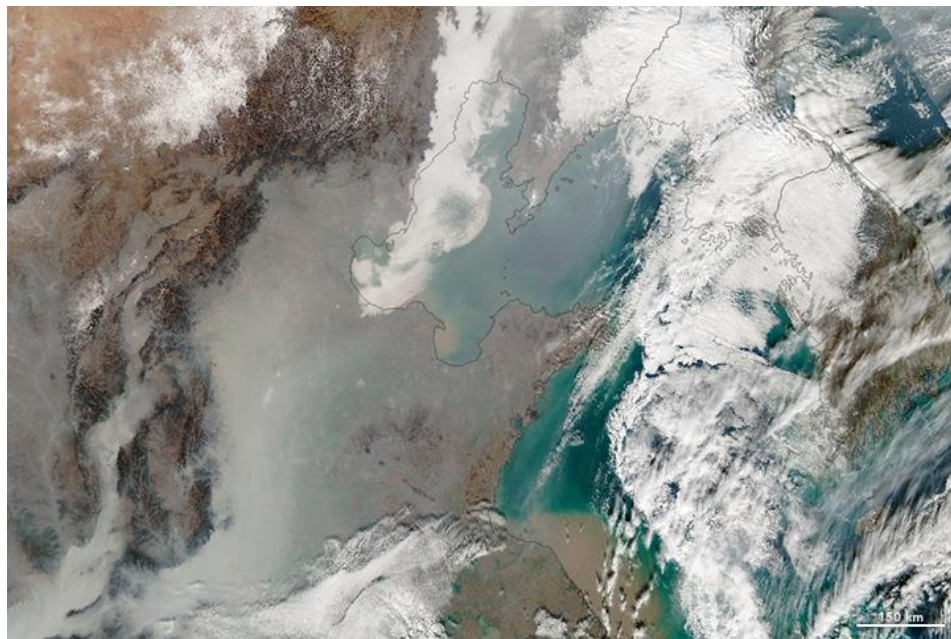


Figure 2 A natural-color image captured by MODIS on the Aqua satellite(NASA Earth Observatory images by Joshua Stevens)

The Jing-Jin-Ji region includes the capital city of Beijing, which is the political, economic and cultural center of China, Tianjin, which is one of the five national central

cities, and Hebei province, which has a strong manufacturing base and steel industries (Pathak, Wu, & Wang, 2009). In April 2017, China announced the establishment of the Xiongan New Area, which is in Hebei province to coordinate the development of the Jing-Jin-Ji region. In this study, AOD of the whole Jing-Jin-Ji region is assessed, and AODs of major Jing-Jin-Ji cities are compared with each other.

Section 3.2 Datasets & Quality assurance

18-year (March 2000 - April 2017) records of aerosol optical depth at $0.55 \mu\text{m}$ obtained from MODIS onboard the Terra satellite are used in this study. The Collection 6 L3 MODIS Aerosol Eight-Day product is chosen, and spatial resolution of it is at $1^\circ \times 1^\circ$. NASA EOS team produces 46 L3 8-day datasets each year. In figure 3, total 29 green shaded grids ($1^\circ \times 1^\circ$) are chosen as the study area.

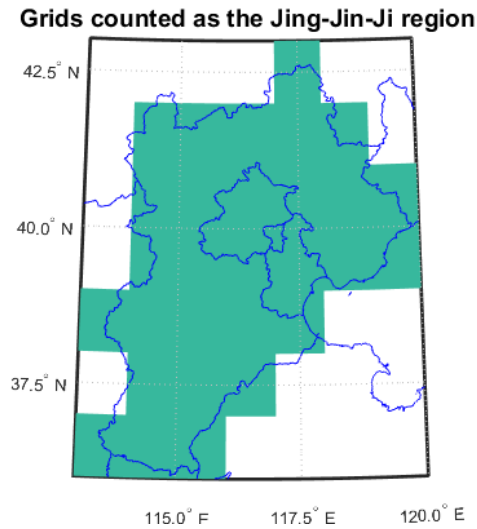


Figure 3 Grids counted as the Jing-Jin-Ji region

Since L3 8-day products are computed from L3 daily products and L3 daily products are derived from the L2 product, the quality of L2 products plays an important role in the quality of the L3 product. To produce L3 with better quality, low-quality L2 data should be avoided during the aggregation.

Because of errors with detectors, bad weather conditions and some problems with algorithms, not all L2 pixels are in good quality. Quality Assurance (QA) flags give an indication of the quality of the data. By giving more weight to more reliable L2 input pixels in the computation of L3, QA weighting of L2 products can reduce the influence of unconfident pixels. The “Corrected aerosol optical depth (Land) at 0.47, 0.55, and 0.66 microns: Mean of Level-3 QA Weighted Mean” is used in this study. From this product, the AOD at 0.55 μm is extracted for AOD analysis.

Section 3.3 Time Series Analysis

Long-term monitoring data has much valuable information included. As described below, suitable time series analysis can extract trends, seasonal and remainder information from long-term time series. In this study, AOD data are considered as a periodic time series.

First, a simple time series plot is presented to give a basic idea about AOD during 2000-2017, and trendlines are included to show the AOD tendency. The mean annual cycle of AOD is calculated to know its seasonal change.

Then, seasonal decomposition is applied. The basic idea of seasonal decomposition is that a time series can be thought of as consisting of three components: a

trend, seasonal effects, and remainders. These components can be combined in an additive or multiplicative way to get the time series (Equation 1).

Equation 1 Additive and multiplicative structures for decomposition models

$$X_t = Trend + Seasonal + Remainder \text{ (Addictive)}$$

$$X_t = Trend * Seasonal * Remainder \text{ (Multiplicative)}$$

X_t is the value of the time series at time t

The first step of seasonal decomposition is to estimate the trend, which can be done by a smoothing procedure and a regression equation. Then, the trend is removed from the series. Next, seasonal effects are estimated by using the de-trended series, which can be done by averaging data for all years. The final step is to get the remainder component.

Seasonal and Trend decomposition using Loess (STL) (Cleveland, Cleveland, & Terpenning, 1990), a robust and versatile time series decomposition method, is applied in this study. And it is realized by the STL function in R.

The AOD trends of four seasons are also discussed. The 46 data intervals of each year are divided into four parts to match with four seasons. Table 1 shows the principles of season's division.

Table 1 The Division of Four Seasons and the Corresponding 8-Day Dataset

Season	Month	8-Day Dataset Order
Winter	December, January & February	43-46 (from last year) & 1-7
Spring	March, April & May	8-19
Summer	June, July & August	20-30
Autumn	September, October & November	31-42

Section 3.4 Spatial Distribution Analysis

First, the mean AOD distribution of the Jing-Jin-Ji region during 2000-2017 is discussed. Then, the AOD grids where Beijing, Tianjin, Tangshan, Shijiazhuang, Xiongan, and Handan are located are collected together for the comparison of AOD values in different seasons. Table 2 lists the names of cities or areas with their longitudes and latitudes.

Table 2 Major cities in the Jing-Jin-Ji region

CITY/AREA	LONGITUDE	LATITUDE
BEIJING	39.9042° N	116.4074° E
TIANJIN	39.3434° N	117.3616° E
TANGSHAN	39.6309° N	118.1802° E
SHIJIAZHUANG	38.0428° N	114.5149° E
XIONGAN	38.9354° N	115.9356° E
HANDAN	36.6257° N	114.5390° E

Section 3.5 Smog Event Detection

Smog is one kind of air pollution, originally named for the mixture of smoke and fog in the air. Smog events frequently occur in the Jing-Jin-Ji region. In this section, several reported smog events are picked to verify if the MODIS 8-day AOD product at the corresponding time could detect the smog. Following are three reported severe and lasting smog events in the North China Plain. The comparison between the AOD product and *in situ* Air Quality Index (AQI) values are made. The AQI level is based on the level of six atmospheric pollutants, namely particulate matter with diameter less than 10 μ m

(PM₁₀), particulate matter with diameter less than 2.5 μ m (PM_{2.5}), sulfur dioxide (SO₂), nitrogen dioxide (NO₂), carbon monoxide (CO), and ozone (O₃) measured at the MEP monitoring stations. An individual AQI (IAQI) of each pollutant is calculated and the highest of those six scores is considered as the final AQI (“People’s Republic of China Ministry of Environmental Protection Standard: Technical Regulation on Ambient Air Quality Index (on trial),” 2012). If the primary pollutant is particulate matter, the AQI is quite related to the load of aerosols in the air. Compared with the AQI which is measured at one certain height per station, the AOD measured by satellite indicates the vertical integral of the aerosol load.

Table 3 Smog events and the duration

Event	Approximate Start Date and End Date
A	November 27th, 2015 – December 2nd, 2015
B	December 16 th , 2016 – December 21 st , 2016
C	December 30 th , 2016 – January 7 st , 2017

CHAPTER 4 DATA ANALYSIS AND FINDINGS

Section 4.1 Trend and Seasonal Cycle

Temporal characteristics of AOD in the Jing-Jin-Ji region are discussed in this section. Figure 4 presents the long-term time series of 8-Day MODIS AOD over the Jing-Jin-Ji region (29 grids) starting from March 2000 to April 2017. The AOD trend has a strong seasonal cycle which increases in the summer and decreases in the winter every year. The linear regression (shown as an orange line) has a positive slope, indicating an increasing AOD trend during 2000-2017. But the fittings with higher degree polynomials such as quadratic fitting (shown as a purple curve) and cubic (shown as a green curve) fitting provide a trend with more details, showing an increasing tendency from 2000 to 2011 and a strong decreasing tendency after 2011.

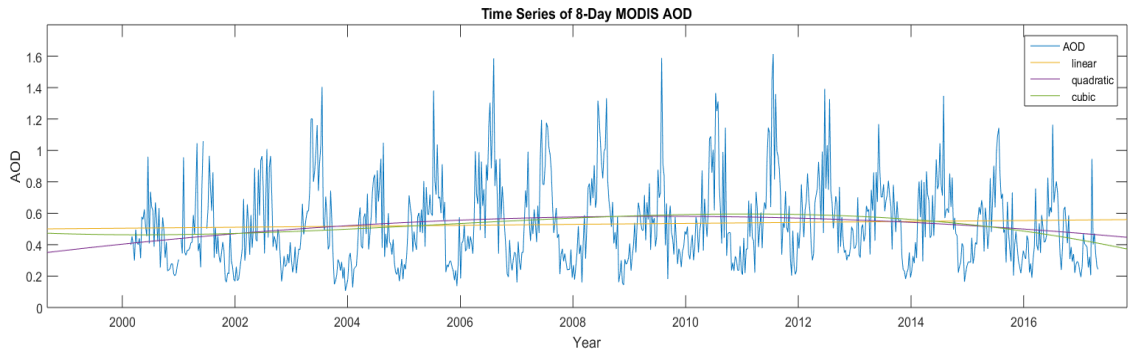


Figure 4 Time series of 8-Day MODIS AOD over the Jing-Jin-Ji region.

The seasonal cycle is presented in Figure 5, which is derived by averaging AOD seasonal cycle over 18 years without considering a trend. The AOD has the highest value in the summer and lowest value in the winter (November, December, and January), while most smog events are reported in the winter. This observation result agrees with previous studies (Jinhuan & Liquan, 2000; Z. Li et al., 2007), and the high AOD in the summer was explained by the high humidity in the summer which could cause the growth of aerosol particles and by the stronger vertical convection in the summer.

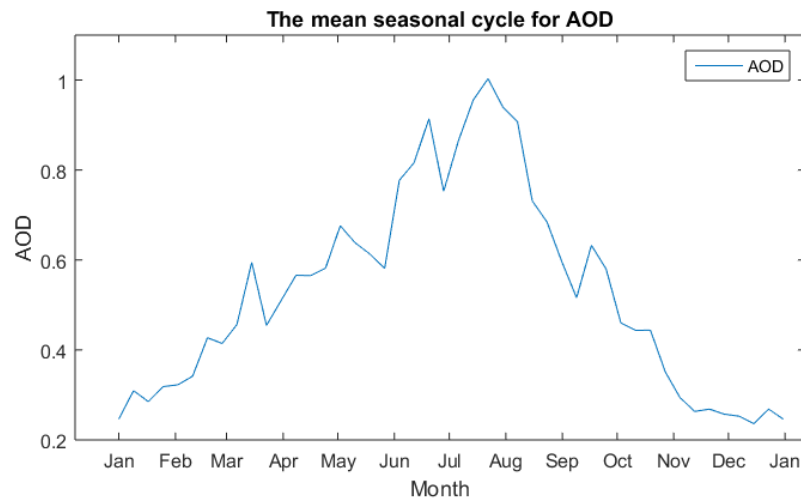


Figure 5 The mean seasonal cycle of 8-Day MODIS AOD over the Jing-Jin-Ji region.

The STL decomposition result is shown in figure 6. The time series is divided into three components. The sum of the three components equals the data time series. The seasonal component is estimated by Loess smoothing of all seasonal sub-series. The decomposed seasonal component has a similar tendency as the calculated seasonal mean (Figure 7). The AOD trend in Figure 6 shows a gradual increasing tendency between

2000 and 2012, and a sharp decrease starting from 2012, indicating the air quality has improved since 2012.

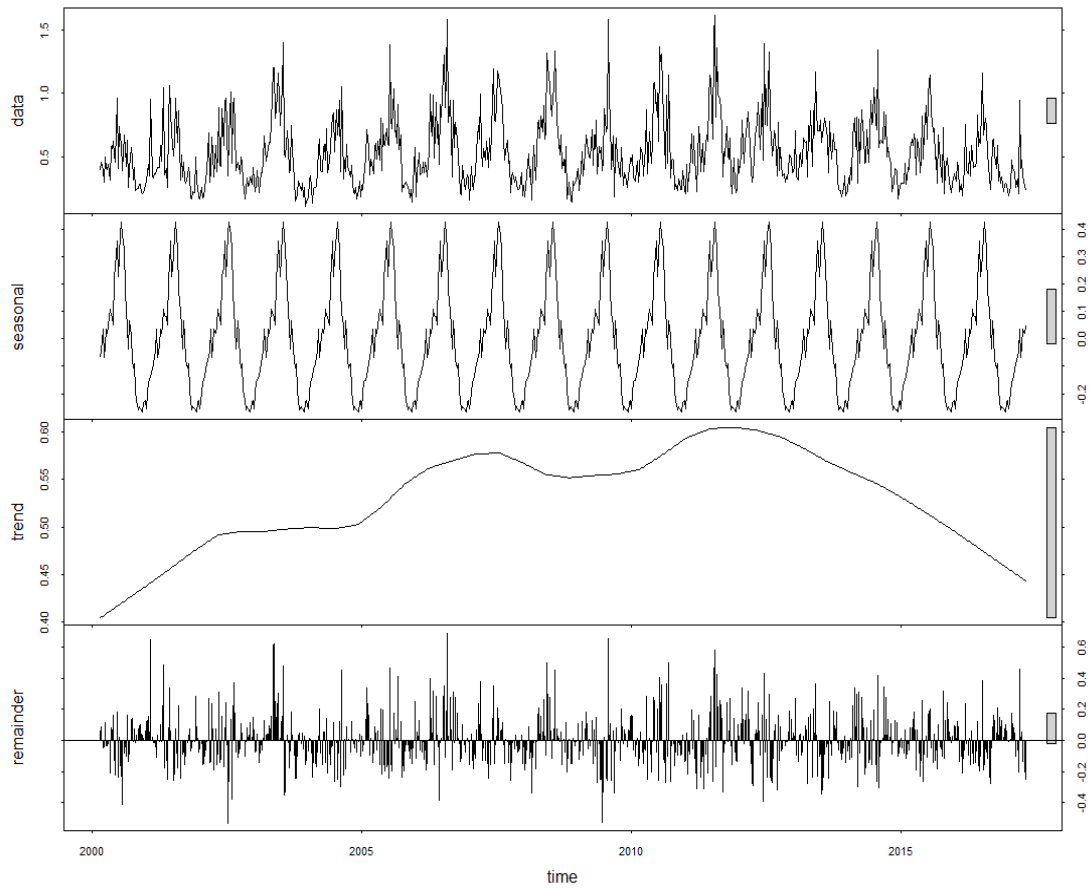


Figure 6 The STL decomposition of an 8-day AOD time series

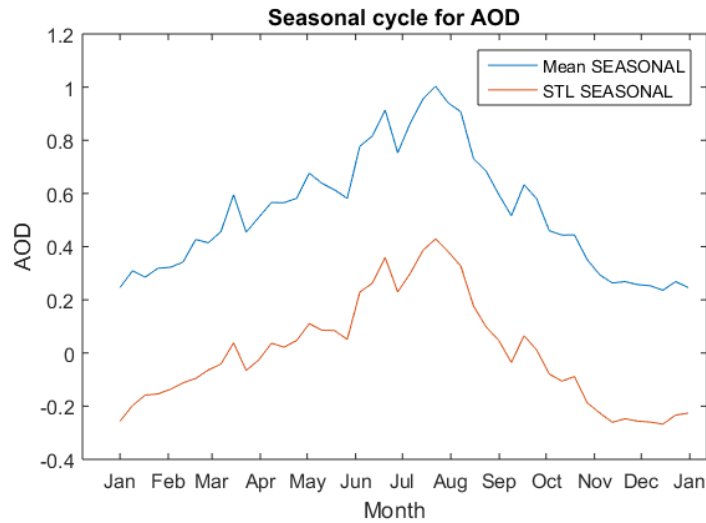


Figure 7 Comparison between STL Seasonal Component and the Mean Seasonal Cycle

The AODs in different seasons are displayed separately in Figure 8. Both the AOD in winter and the AOD in autumn have linear trendlines with increasing tendency. Although no strong linear tendency (orange line) could be seen in spring and summer, the AOD in spring starts to decrease from 2012(blue line), and the AOD in summer has been decreasing rapidly since 2011(blue line). Earlier trend analysis results (Figure 4 and Figure 6) show that the overall AOD is more likely to have a strong decreasing tendency after 2012. However, there is no strong tendency seen in spring and in summer between 2011 and 2016. It is possible that the recent downward trend might be confined to spring and summer which make the greatest contributions to the decreasing tendency from 2012.

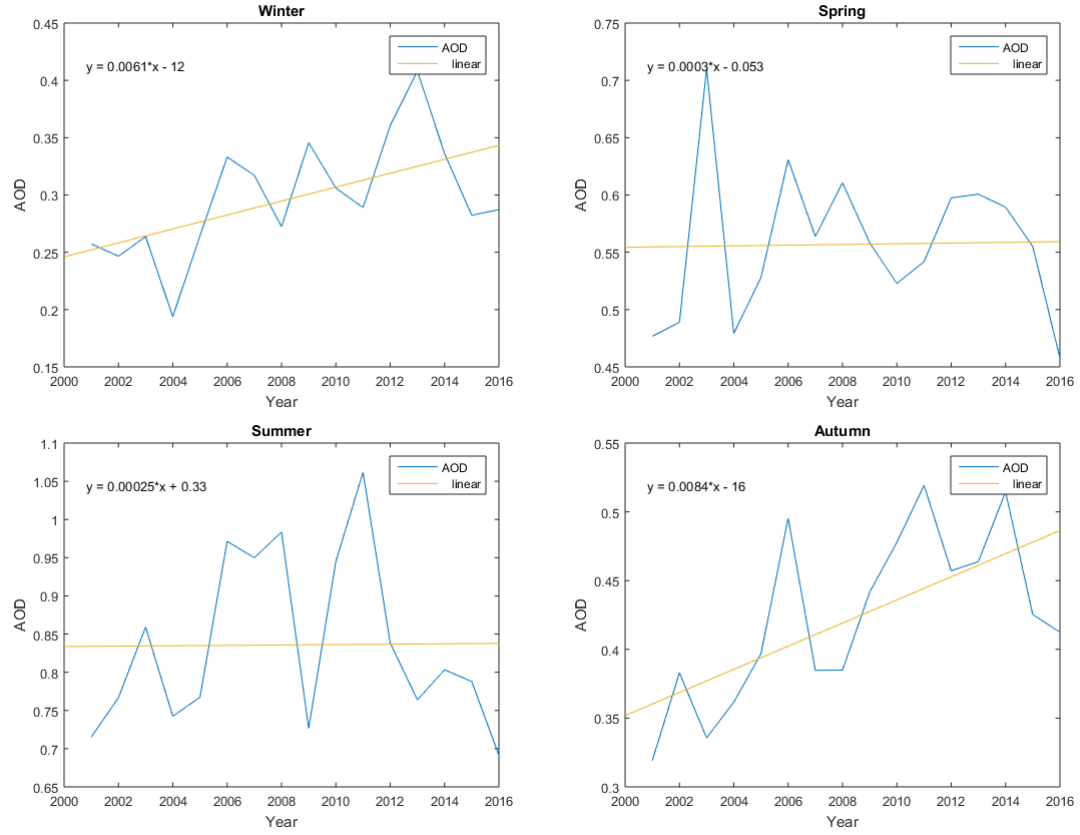


Figure 8 The AOD trends of four seasons

Assuming there is no missing data, each year should have 46 8-day AOD datasets.

For the year 2000 and 2017, an AOD dataset with the same format but NaN value is adopted to replace missing data, which could guarantee every year has 46 8-day AOD datasets. Therefore, there are 18 7datasets corresponding to the same 8-day period but different years.

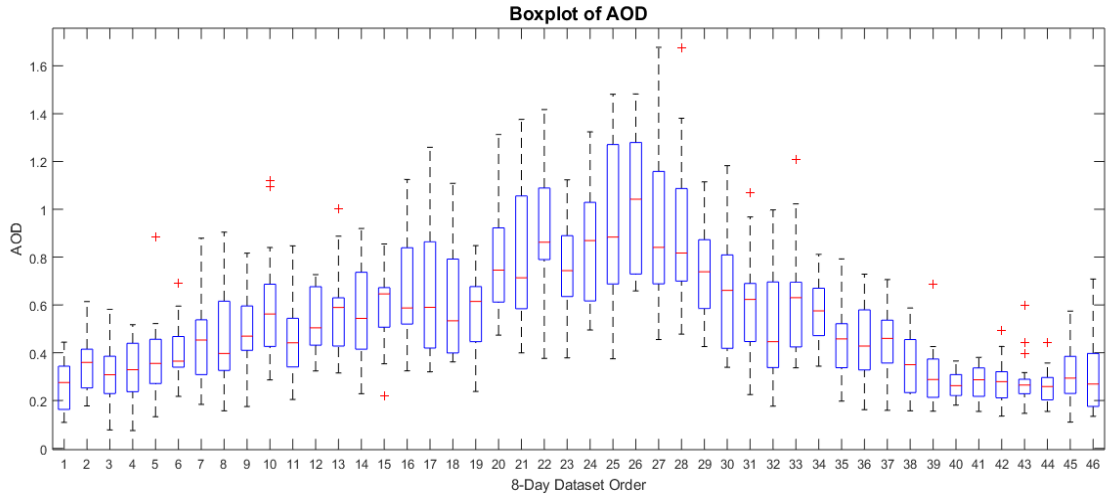


Figure 9 Boxplot of AOD

The boxplot for 46 AOD 8-day groups is presented in Figure 9. Shown by a red line that divides the box into two parts, the median marks the mid-point of the dataset. In this plot, the median shares a similar trend pattern with the AOD mean seasonal cycle. The middle box represents the middle 50% of AOD for that group. The 25th percentile, known as the lower quartile, is shown as the bottom of the box, telling that 25% percent of AOD are below the bottom. And the 75th percentile (the upper quartile), shown as the top of the box, tells that 25% percent of AOD in that group are above the top. In the winter, the box plots are shorter than that in other seasons, indicating that winter's 8-day AODs in different years have a higher level of agreement with each other. From two sides of the box, the whiskers are extended to the data point that is no more than $1.5 \times$ Interquartile (Interquartile = Upper Quartile – Lower Quartile), corresponding to 99.3% coverage of the data for a normal distribution. Beyond the whiskers, outlier data is plotted as a red cross. The range of whiskers is smaller in the winter, similar to the height of the

middle box. The position of the median in the box could tell the distribution of data. If the median does not locate in the middle of the box, it's likely that the data is not normally distributed. This skewness happens frequently between group 6 to 35 (February to October).

Section 4.2 Spatial Distribution

The overview of AOD distribution for the whole region and the whole period are presented in Figure 10. The AOD value of each grid is the average of AOD in that grid over the whole period. The north and northwest parts of the Jing-Jin-Ji region have lower AOD, whereas the southeast and especially south contribute high AOD (above 0.8). The neighboring Shandong province in the south of the Jing-Jin-Ji also has high AOD.

AOD Mean over the Jing-Jin-Ji region and surrounding areas during 2000-2017

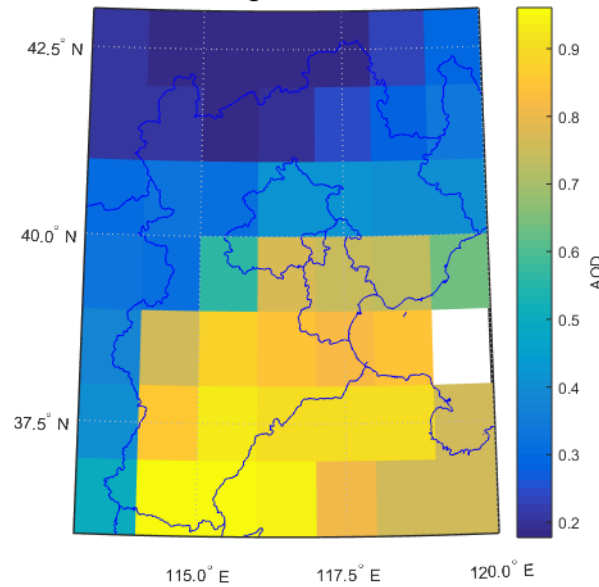


Figure 10 Grids counted as the Jing-Jin-Ji region

The six major cities/areas (shown as a red cross) are selected as study areas for AOD in the small-scale region, and they match with the yellow grids in Figure 11.

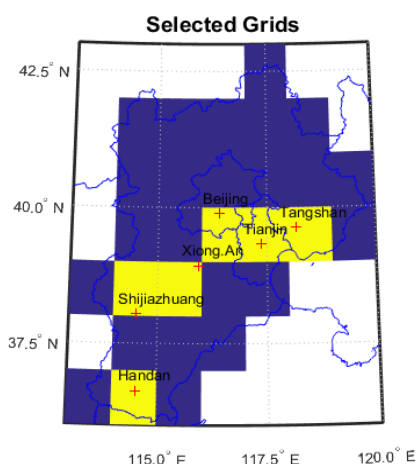


Figure 11 Grids selected for specific cities/areas

Due to the large volume of data, 46 datasets of each year are divided into four parts to match with four seasons, and the AOD mean of each season is calculated. Taking AOD of December 2000 in its winter season dataset, the year 2001 is the starting point. The yearly AOD of four seasons is displayed in Figure 12. Compared with other seasons, summer has the highest AOD for most of the cities/areas. Handan, the industrial city of Hebei province located in the south of the Jing-Jin-Ji region, has the highest AOD in four seasons compared with other cities. Having city's center located between 39° and 40°N; three neighboring cities Beijing, Tianjin, and Tangshan share a similar AOD trend. No strong AOD difference could be found along the west-east direction. However, the cities located in lower latitudes have larger AOD compared with cities in the north. Table 4 lists the AOD values averaged over four-year intervals.

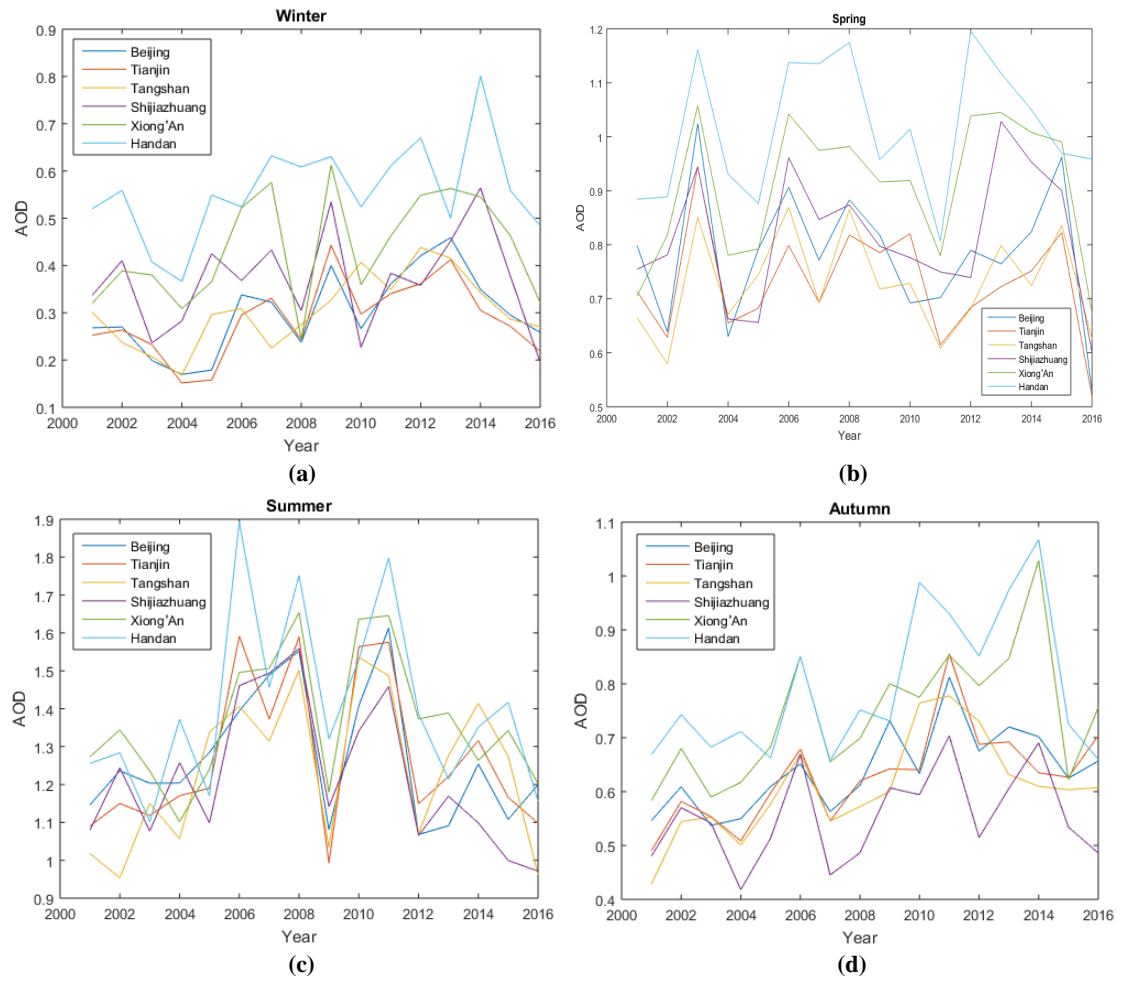


Figure 12 The yearly AOD of four seasons

Table 4 Major cities' AOD mean

Year	Beijing				Tianjin				Tangshan			
	Winter	Spring	Summer	Autumn	Winter	Spring	Summer	Autumn	Winter	Spring	Summer	Autumn
2001-2004	0.23	0.77	1.20	0.56	0.23	0.74	1.13	0.53	0.23	0.69	1.04	0.51
2005-2008	0.27	0.84	1.43	0.61	0.26	0.75	1.44	0.61	0.28	0.79	1.39	0.59
2009-2012	0.36	0.75	1.29	0.71	0.36	0.73	1.32	0.71	0.38	0.68	1.28	0.72
2013-2016	0.34	0.77	1.16	0.68	0.30	0.70	1.20	0.66	0.33	0.75	1.23	0.61
Mean	0.30	0.78	1.27	0.64	0.29	0.73	1.27	0.63	0.30	0.73	1.24	0.61
Year	Shijiazhuang				Xiong'An				Handan			
	Winter	Spring	Summer	Autumn	Winter	Spring	Summer	Autumn	Winter	Spring	Summer	Autumn
2001-2004	0.32	0.79	1.16	0.50	0.35	0.84	1.24	0.62	0.46	0.97	1.25	0.70
2005-2008	0.38	0.83	1.40	0.53	0.43	0.95	1.47	0.72	0.58	1.08	1.57	0.73
2009-2012	0.38	0.77	1.25	0.60	0.50	0.91	1.46	0.81	0.61	0.99	1.51	0.88
2013-2016	0.40	0.87	1.06	0.58	0.47	0.93	1.30	0.81	0.59	1.02	1.28	0.86
Mean	0.37	0.81	1.22	0.55	0.44	0.91	1.37	0.74	0.56	1.02	1.40	0.79

Section 4.3 Air Quality & MODIS 8-Day AOD Product

Since the AOD product's temporal resolution is 8 day, duration of smog is considered as an important factor during smog event collection. Three major smog events with the duration reported longer than 5 days by media are picked for the experiments. Table 5 lists three sub-tables, which match with the three smog events. In the sub-table, the third row is the date, and the fourth row is the daily average AQI. Due to the limited amount of historical AQI, the AQI here was calculated by AQI measured in Beijing sites. The color in the fifth row shows the five levels of health concern related to AQI value. The consecutive pink colored numbers are considered as smog events. The second row gives time ranges of the 8-day AOD product. The duration of Event A is short and is wholly within an 8-day range. For Event B, two AOD intervals cover the event. As with Event B, Event C is related to two AOD intervals, which have overlapped time ranges.

Table 5 The smog event duration, AQI and AOD data time range

Event A																				
AOD Time Range	11/25/2015 - 12/2/2015																			
Date	11/24	11/25	11/26	11/27	11/28	11/29	11/30	12/1	12/2	12/3	12/4	12/5								
AQI	55	72	48	256	310	300	356	473	32	25	41	70								
AQI LEVEL																				
Event B																				
AOD Time Range	12/10/2016 - 12/17/2016 12/18/2016 - 12/25/2016																			
Date	12/8	12/9	12/10	12/11	12/12	12/13	12/14	12/15	12/16	12/17	12/18	12/19	12/20	12/21	12/22	12/23	12/24	12/25	12/26	12/27
AQI	132	36	66	209	225	77	39	52	142	236	273	269	416	430	120	48	157	191	66	56
AQI LEVEL																				
Event C																				
AOD Time Range	12/26/2016 - 1/2/2017 Overlap region 1/1/2017 - 1/8/2017																			
Date	12/24	12/25	12/26	12/27	12/28	12/29	12/30	12/31	1/1	1/2	1/3	1/4	1/5	1/6	1/7	1/8	1/9	1/10		
AQI	157	191	66	56	96	75	259	340	467	258	340	399	275	247	216	56	49	42		
AQI LEVEL																				
Good Moderate Unhealthy for Sensitive Groups Unhealthy Very Unhealthy Hazardous																				

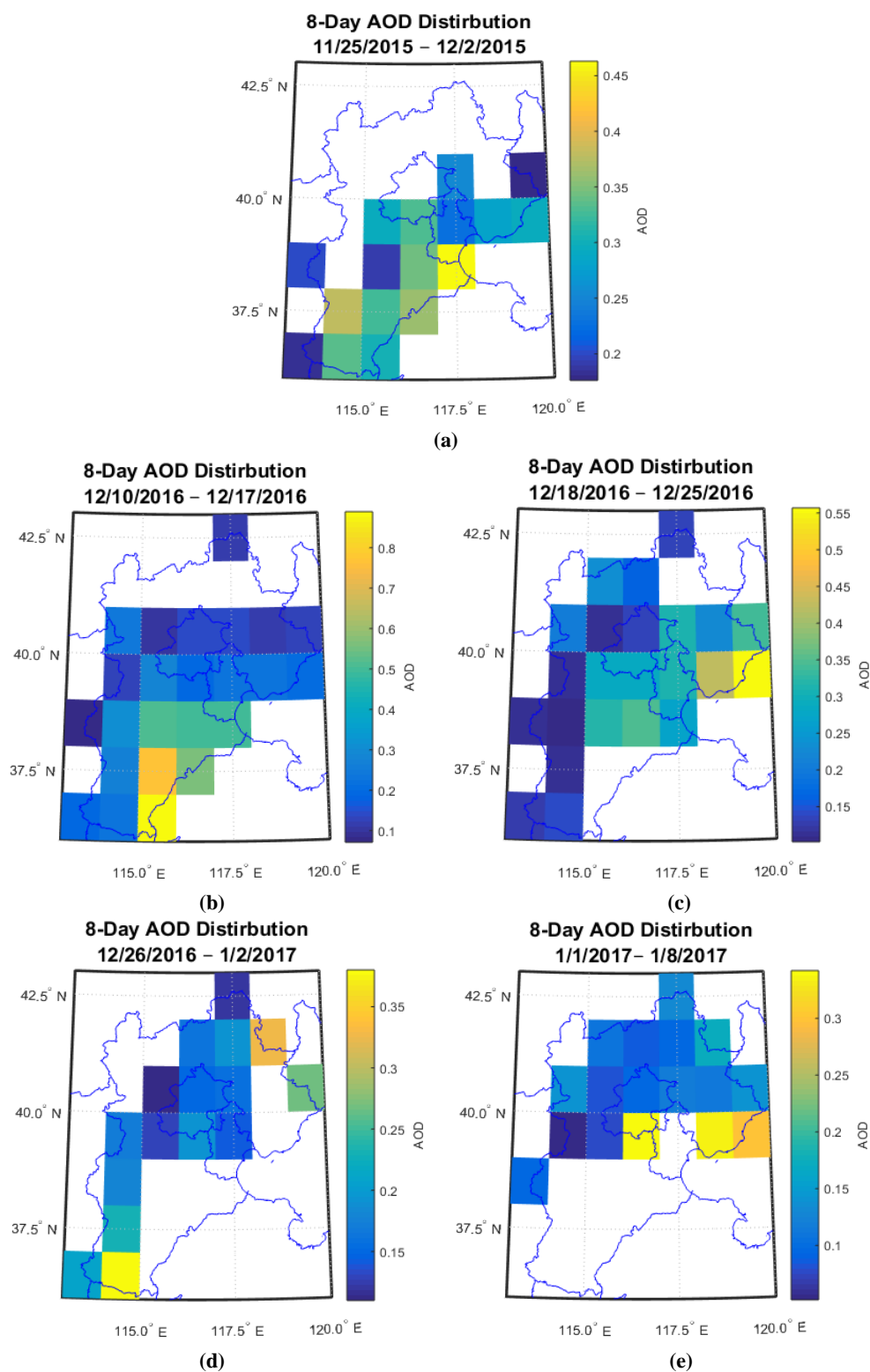
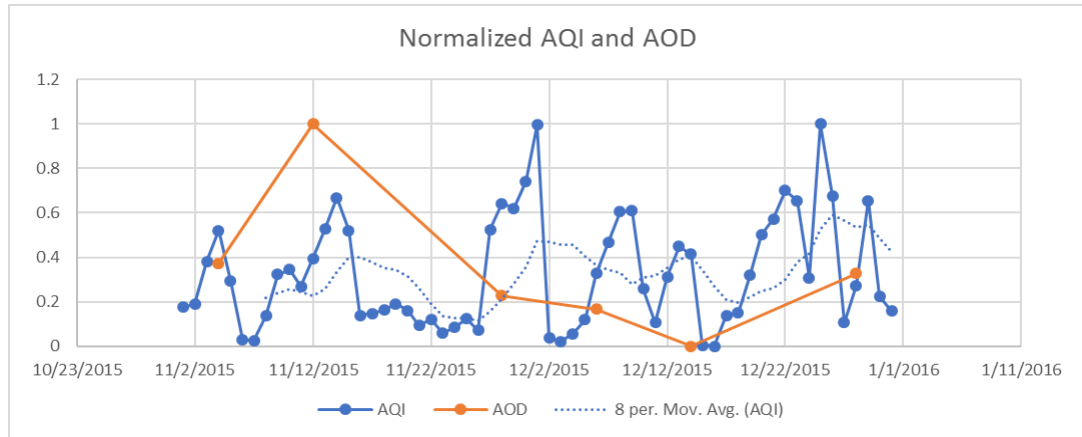
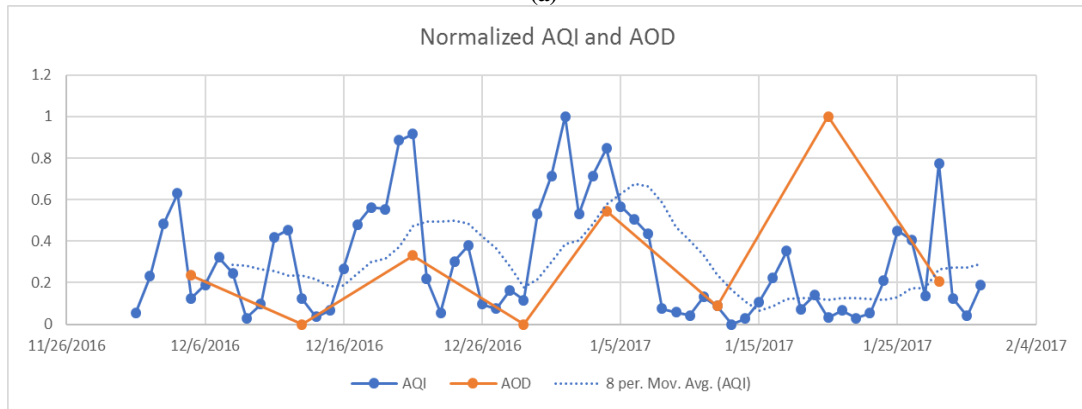


Figure 13 AOD products involved when smog events happened

Five corresponding AOD 8-Day products are displayed in Figure 13. All of them have missing data, which might be caused by cloud. Due to the missing values, the comparison between two consecutive AOD products cannot be done because only a few of the grids have valid AOD value in two products. Since the historical AQI data of Beijing is available online (<https://www.aqistudy.cn/historydata/>) and Beijing's grid has AOD available for five products, comparisons between Beijing's AQI value and its AOD value are done. The absolute value of AOD is always much smaller than AQI as the units are different, so Min-Max normalization is applied to aid the trend comparison between AQI and AOD (Figure 13). Comparison of AQI and AOD are made for the data acquired between November 2015 to December 2015 (Figure 14(a)) and between December 2016 and January 2017 (Figure 14(b)).



(a)



(b)

Figure 14 Normalized AQI and AOD

Since AQI data has a one-day temporal resolution but AOD has an 8-day resolution. To match with AOD, a moving average for AQI with 8 as the period is applied. The moving average trend line is shown as a blue dotted line. The overall tendency of AOD and AQI moving average is very similar, except on 11/25/2015 when AOD is decreasing but AQI is increasing and on 1/20/2017 when AOD has high extremum value while AQI has no increasing or decreasing tendency.

Among these three major smog events, smog event A cannot be recognized from the AOD data. Maxima show in the AOD trend when smog events B and C happened.

However, if 8-day AOD is the only data source, then the point on 1/20/2017 is more likely to be interpreted as smog events, which could mislead the interpretation.

CHAPTER 5 CONCLUSIONS AND DISCUSSION

The time series of AOD in the Jing-Jin-Ji region indicates a strong season cycle, which has a peak in summer and the lowest point in winter. The AOD values among different years are more consistent in winter, while AOD values have the largest variability in summer. Though the linear trendline shows a positive slope; the quadratic and cubic trendlines, and the trend computed by seasonal decomposition show a decreasing trend after the year 2012. Both AOD values in winter and in autumn have an increasing tendency, and AOD values in summer and in spring after 2011 might make the greatest contribution to the recent downward trend. The AOD values in the southern part of the Jing-Jin-Ji region are larger than them in the north.

Long-lasting smog events can be seen in the AOD 8-day products, but a correct interpretation requires the consideration of many other factors. For example, the vertical distribution of aerosols is valuable for getting a better estimation of ground-level air quality. Light Detection and Ranging (LIDAR) might be a useful tool for achieving this improvement. Also, the AOD information from the ground-based aerosol monitoring network, such as AErosol RObotic NETwork(AERONET), can be used to fill missing data of MODIS 8-day AOD products. In addition, higher temporal resolution of AOD could be helpful for detecting smog events with short periods.

REFERENCES

- Ackerman, S. A., Strabala, K. I., Menzel, W. P., Frey, R. A., Moeller, C. C., & Gumley, L. E. (1998). Discriminating clear sky from clouds with MODIS. *Journal of Geophysical Research: Atmospheres*, 103(D24), 32141–32157.
<https://doi.org/10.1029/1998JD200032>
- Andreae, M. O., & Rosenfeld, D. (2008). Aerosol–cloud–precipitation interactions. Part 1. The nature and sources of cloud-active aerosols. *Earth-Science Reviews*, 89(1–2), 13–41. <https://doi.org/10.1016/j.earscirev.2008.03.001>
- Chu, D. A., Kaufman, Y. J., Zibordi, G., Chern, J. D., Mao, J., Li, C., & Holben, B. N. (2003). Global monitoring of air pollution over land from the Earth Observing System-Terra Moderate Resolution Imaging Spectroradiometer (MODIS). *Journal of Geophysical Research: Atmospheres*, 108(D21), 4661.
<https://doi.org/10.1029/2002JD003179>
- Cleveland, R. B., Cleveland, W. S., & Terpenning, I. (1990). STL: A Seasonal-Trend Decomposition Procedure Based on Loess. *Journal of Official Statistics; Stockholm*, 6(1), 3.
- Dudhia, J., Ruiz-Arias, A., Gueymard, A., & Pozo-Vazquez, D. (2013). Assessment of the Level-3 MODIS daily aerosol optical depth in the context of surface solar

- radiation and numerical weather modeling. *Atmospheric Chemistry and Physics*, 13(2), 675. <https://doi.org/10.5194/acp-13-675-2013>
- Engel-Cox, J. A., Holloman, C. H., Coutant, B. W., & Hoff, R. M. (2004). Qualitative and quantitative evaluation of MODIS satellite sensor data for regional and urban scale air quality. *Atmospheric Environment*, 38(16), 2495–2509. <https://doi.org/10.1016/j.atmosenv.2004.01.039>
- Forster, P., Ramaswamy, V., Artaxo, P., Berntsen, T., Betts, R., Fahey, D. W., ... Van Dorland, R. (2007). Changes in Atmospheric Constituents and in Radiative Forcing. Chapter 2. Retrieved from http://inis.iaea.org/Search/search.aspx?orig_q=RN:39002468
- Fu, L., Wan, W., Zhang, W., & Cheng, H. (2016). China Air 2016– Air Pollution Prevention and Control Progress in Chinese Cities.
- Hao, J., & Wang, L. (2005). Improving Urban Air Quality in China: Beijing Case Study. *Journal of the Air & Waste Management Association*, 55(9), 1298–1305. <https://doi.org/10.1080/10473289.2005.10464726>
- Hubanks, P., Platnick, S., King, M., & Ridgway, B. (2016). MODIS Atmosphere L3 Gridded Product Algorithm Theoretical Basis Document for C6.
- Ji, D., Wang, Y., Wang, L., Chen, L., Hu, B., Tang, G., ... Liu, Z. (2012). Analysis of heavy pollution episodes in selected cities of northern China. *Atmospheric Environment*, 50, 338–348. <https://doi.org/10.1016/j.atmosenv.2011.11.053>

- Jinhuan, Q., & Liquan, Y. (2000). Variation characteristics of atmospheric aerosol optical depths and visibility in North China during 1980–1994. *Atmospheric Environment*, 34(4), 603–609. [https://doi.org/10.1016/S1352-2310\(99\)00173-9](https://doi.org/10.1016/S1352-2310(99)00173-9)
- Johnson, I. (2015, July 19). As Beijing Becomes a Supercity, the Rapid Growth Brings Pains. *The New York Times*. Retrieved from <https://www.nytimes.com/2015/07/20/world/asia/in-china-a-supercity-rises-around-beijing.html>
- Kaufman, Y. J., & Fraser, R. S. (1983). Light Extinction by Aerosols during Summer Air Pollution. *Journal of Climate and Applied Meteorology*, 22(10), 1694–1706. [https://doi.org/10.1175/1520-0450\(1983\)022<1694:LEBADS>2.0.CO;2](https://doi.org/10.1175/1520-0450(1983)022<1694:LEBADS>2.0.CO;2)
- King, M. D., Byrne, D. M., Herman, B. M., & Reagan, J. A. (1978). Aerosol Size Distributions Obtained by Inversions of Spectral Optical Depth Measurements. *Journal of the Atmospheric Sciences*, 35(11), 2153–2167. [https://doi.org/10.1175/1520-0469\(1978\)035<2153:ASDOBI>2.0.CO;2](https://doi.org/10.1175/1520-0469(1978)035<2153:ASDOBI>2.0.CO;2)
- King, M. D., Kaufman, Y. J., Tanré, D., & Nakajima, T. (1999). Remote Sensing of Tropospheric Aerosols from Space: Past, Present, and Future. *Bulletin of the American Meteorological Society*, 80(11), 2229–2259. [https://doi.org/10.1175/1520-0477\(1999\)080<2229:RSOTAF>2.0.CO;2](https://doi.org/10.1175/1520-0477(1999)080<2229:RSOTAF>2.0.CO;2)
- Klingmüller, K., Pozzer, A., Metzger, S., Stenchikov, G. L., & Lelieveld, J. (2016). Aerosol optical depth trend over the Middle East. *Atmos. Chem. Phys.*, 16(8), 5063–5073. <https://doi.org/10.5194/acp-16-5063-2016>

- Lee, K. H., Li, Z., Kim, Y. J., & Kokhanovsky, A. (2009). Atmospheric Aerosol Monitoring from Satellite Observations: A History of Three Decades. In P. D. Y. J. Kim, P. D. U. Platt, D. M. B. Gu, & D. H. Iwahashi (Eds.), *Atmospheric and Biological Environmental Monitoring* (pp. 13–38). Springer Netherlands.
https://doi.org/10.1007/978-1-4020-9674-7_2
- Li, W., Zhou, S., Wang, X., Xu, Z., Yuan, C., Yu, Y., ... Wang, W. (2011). Integrated evaluation of aerosols from regional brown hazes over northern China in winter: Concentrations, sources, transformation, and mixing states. *Journal of Geophysical Research: Atmospheres*, 116(D9), D09301.
<https://doi.org/10.1029/2010JD015099>
- Li, Z., Xia, X., Cribb, M., Mi, W., Holben, B., Wang, P., ... Dickerson, R. E. (2007). Aerosol optical properties and their radiative effects in northern China. *Journal of Geophysical Research: Atmospheres*, 112(D22), D22S01.
<https://doi.org/10.1029/2006JD007382>
- Pathak, R. K., Wu, W. S., & Wang, T. (2009). Summertime PM_{2.5} ionic species in four major cities of China: nitrate formation in an ammonia-deficient atmosphere. *Atmos. Chem. Phys.*, 9(5), 1711–1722. <https://doi.org/10.5194/acp-9-1711-2009>
- People's Republic of China Ministry of Environmental Protection Standard: Technical Regulation on Ambient Air Quality Index (on trial). (2012). China's Ministry of Environmental Protection.

- Platnick, S. (2015). MODIS Atmosphere L3 Eight-Day Product. NASA MODIS Adaptive Processing System, Goddard Space Flight Center. Retrieved from http://dx.doi.org/10.5067/MODIS/MOD08_E3.006
- Pope, C. A. I., Ezzati, M., & Dockery, D. W. (2009). Fine-Particulate Air Pollution and Life Expectancy in the United States. *New England Journal of Medicine*, 360(4), 376–386. <https://doi.org/10.1056/NEJMsa0805646>
- Prasad, A. K., Singh, R. P., & Singh, A. (2004). Variability of aerosol optical depth over indian subcontinent using modis data. *Journal of the Indian Society of Remote Sensing*, 32(4), 313. <https://doi.org/10.1007/BF03030855>
- Remer, L. A., Kaufman, Y. J., Tanré, D., Mattoo, S., Chu, D. A., Martins, J. V., ... Holben, B. N. (2005). The MODIS Aerosol Algorithm, Products, and Validation. *Journal of the Atmospheric Sciences*, 62(4), 947–973. <https://doi.org/10.1175/JAS3385.1>
- Remer, Lorraine A., Kleidman, R. G., Levy, R. C., Kaufman, Y. J., Tanré, D., Mattoo, S., ... Holben, B. N. (2008). Global aerosol climatology from the MODIS satellite sensors. *Journal of Geophysical Research: Atmospheres*, 113(D14), D14S07. <https://doi.org/10.1029/2007JD009661>
- Wang, J., & Christopher, S. A. (2003). Intercomparison between satellite-derived aerosol optical thickness and PM_{2.5} mass: Implications for air quality studies. *Geophysical Research Letters*, 30(21), 2095. <https://doi.org/10.1029/2003GL018174>

Xie, T., Wang, L., Ling, X., Shen, X., Wang, M., & Tianyang, F. (2015). China Air Quality Management Assessment Report(2015).

Zhang, Q., He, K., & Huo, H. (2012). Policy: Cleaning China's air. *Nature*, 484(7393), 161–162. <https://doi.org/10.1038/484161a>

Zhao, Y. (2017, March 6). Air quality improved in more cities: MEP. Retrieved May 11, 2017, from http://english.sepa.gov.cn/News_service/media_news/201703/t20170306_398203.shtml

BIOGRAPHY

Xiqi Fei graduated from The High School Attached to Zhejiang University in 2011. She received her Bachelor of Engineering from the China University of Geosciences in 2015. She worked as a research assistant for USDA Economic Research Service Center in 2017. Her Master studies at George Mason University majoring in Earth System Science will be finished by May 2017.